Electrical conductivity enhanced dielectric and ferroelectric properties of interface-coupled ferroelectric superlattices

Y. Zhou[a)]
Department of Applied Physics, The Hong Kong Polytechnic University, Hong Kong

F. G. Shin
Department of Applied Physics, Materials Research Center and Center for Smart Materials, The Hong Kong Polytechnic University, Hong Kong

(Received 11 January 2006; accepted 9 April 2006; published online 18 July 2006)

We have developed a model to theoretically study the interplay of the effects of interfacial coupling and electrical conductivity on the ferroelectric and dielectric properties of superlattices consisting of alternating ferroelectric and paraelectric layers based on the Landau-Ginzburg theory. The qualitative predictions of the model are compared with recent experimental results for "symmetric" and "asymmetric" superlattices. It is shown that the consideration of time-dependent space-charge-limited conductivity and "interface structure" can satisfactorily account for the enhancement of the overall ferroelectric and dielectric properties of ferroelectric-paraelectric superlattices. © *2006 American Institute of Physics*. [DOI: 10.1063/1.2208307]

I. INTRODUCTION

Recently, the investigations of ferroelectric multilayer/superlattices have received considerable attention due to the fact that these kinds of materials have been identified as possessing functional physical properties in a sense more superior than their single-phase constituent films.[1–3] The most commonly observed anomalous phenomenon of ferroelectric superlattices is that the remanent polarization is much larger than their single-phase thin films. Lee *et al.* reported a strong polarization enhancement in three-component ferroelectric superlattices.[3] Shimuta *et al.* reported the largest remanent polarization $2P_r$ of 46 $\mu C/cm^2$, which is about three times that of the $BaTiO_3$ single-phase film, in asymmetric strained superlattice structures consisting of alternating $BaTiO_3$ (BTO) and $SrTiO_3$ (STO) with different layer thicknesses.[1] The enhancement in the dielectric constant is also a commonly observed phenomenon in ferroelectric multilayer/superlattices. Pontes *et al.* reported 45% enhancement of the dielectric constant in multilayered $Pb(Zr_{0.6}Ti_{0.4})O_3/Pb(Zr_{0.4}Ti_{0.6})O_3$ thin films grown by a chemical solution route.[2] Xu *et al.* observed an enhanced dielectric constant of 660 at 1 kHz for the polycrystalline $BaTiO_3/SrTiO_3$ with a stacking periodicity of 66 nm.[4] In addition, recent results have shown that the ferroelectric and dielectric properties are sensitively dependent on various macroscopic geometrical parameters such as layer thickness, layering sequence, and individual layer thickness ratio.[1,5]

As far as theory is concerned, it is generally believed that the interfacial coupling between the constituent layers should play an important role and hence must be taken into consideration.[6,7] Typically, the ferroelectric and dielectric properties of the superlattices depend sensitively on the interfacial coupling between individual component layers as found by Qu *et al.* based on a Landau-like phenomenological theory.[7] On the other hand, it has been demonstrated that electrical conductivity in ferroelectric thin films could be responsible for quite a few anomalous ferroelectric and dielectric behaviors, which may be difficult to understand if the materials are regarded as perfectly insulating.[8–11] In particular, the time-dependent space-charge-limited (TDSCL) conduction has been demonstrated to be a possible origin leading to the abnormal polarization offset along the polarization axis widely observed in the compositionally graded ferroelectric multilayers.[8,9] However, further theoretical understanding of the ferroelectric and dielectric behaviors of the multilayer/superlattice stucture is still greatly needed, particularly at a fundamental level. In addition, so far only very few theoretical investigations have been performed to study the interplay of the effects of interfacial coupling and electrical conductivity on the ferroelectric and dielectric properties of the superlattices.

Motivated by the technological interest of ferroelectric superlattices for device applications, we aim in the present work to study the effects of interface structure and electrical conductivity to gain a good understanding of the intriguing properties of ferroelectric superlattices. The calculated trends of the properties (i.e., the intrinsic average polarization and dielectric response, the remanent polarization, and permittivity of the superlattice under dynamic measurements) are compared with recent experimental observations.

II. THEORY AND MODELING

Consider an infinite ferroelectric superlattice formed from alternating layers of two different materials A and B (see Fig. 1). A typical repeating unit (a period) of this structure is a bilayer of A and B. Periodic boundary conditions are applied to the top and bottom surfaces of this bilayer unit so as to describe the infinite ferroelectric superlattice. This suggests that we only have to consider a one-period superlattice

[a)]Electronic mail: yanzhouy@hotmail.com

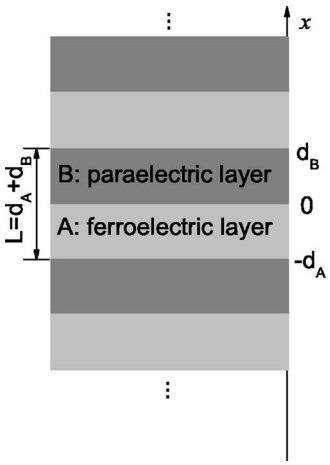

FIG. 1. Schematic diagram of the ferroelectric-paraelectric superlattice structure in our model; d_A and d_B denote the ferroelectric and paraelectric layer thicknesses, respectively.

structure. Furthermore, each layer A or B in the superlattice interacts with its neighboring layers via some interfacial coupling mechanism to be elaborated later on.

We assume that all spatial variations take place along the normal x direction. The dynamics of the dipoles of A and B are modeled by the Landau-Khalatnikov equation:

$$\gamma_A \frac{\partial P_A(x,t)}{\partial t} = -\alpha_A P_A(x,t) - \beta_A P_A(x,t)^3 + E_A(x,t) + \kappa_A \frac{d^2 P_A(x,t)}{dx^2},$$

$$\gamma_B \frac{\partial P_B(x,t)}{\partial t} = -\alpha_B P_B(x,t) - \beta_B P_B(x,t)^3 + E_B(x,t) + \kappa_B \frac{d^2 P_B(x,t)}{dx^2}, \tag{1}$$

where γ represents the viscosity that causes the delay in motion of dipole moments. α and β are the corresponding Landau coefficients of the material. For simplicity we retained in the relevant Landau free energy only terms up to the fourth power of the polarization. The last term in each of the above equations comes from energy associated with polarization gradients, where κ is the corresponding interaction coefficient between neighboring dipoles. $E(x,t)$ is the electric field at location x and time t.

In equilibrium, the stable state of the ferroelectric superlattice is obtained from Eq. (1) as follows:

$$\kappa_A \frac{d^2 P_A(x)}{dx^2} = \alpha_A P_A(x) + \beta_A P_A(x)^3 - E_A(x),$$

$$\kappa_B \frac{d^2 P_B(x)}{dx^2} = \alpha_B P_B(x) + \beta_B P_B(x)^3 - E_B(x). \tag{d2}$$

The corresponding dielectric susceptibility is often found by taking the differentiation of Eq. (2):

$$\kappa_A \frac{d^2 \chi_A(x)}{dx^2} = \alpha_A \chi_A(x) + 3\beta_A P_A^2(x)\chi_A(x) - \frac{1}{\varepsilon_0},$$

$$\kappa_B \frac{d^2 \chi_B(x)}{dx^2} = \alpha_B \chi_B(x) + 3\beta_B P_B^2(x)\chi_B(x) - \frac{1}{\varepsilon_0}, \tag{d3}$$

where χ is taken to be defined by $\varepsilon_0 \chi \equiv \partial P / \partial E$.

The form of the kinetic equations above conforms to the equations used by a number of works, notedly,[12,13] which is obtained by minimizing the free energy of the film under applied electric field. It should be noted that $E(x,t)$ in Eqs. (1) and (2) denotes the local electric field instead of external electric field [see Eq. (12)]. With this approach, the explicit consideration of the depolarization field is subsumed in the formulation. In particular, Baudry and Tournier[12] have given an excellent discussion on this point, incorporating implications due to the presence of charge carriers and nonuniformity of polarization.

Taking interfacial coupling between layers A and B into account,[14,15] the boundary conditions for the polarizations at the interfaces $x=0$ are

$$\kappa_A \left.\frac{dP_A}{dx}\right|_{x=0} - \lambda[P_A(0) - P_B(0)] = 0,$$

$$\kappa_B \left.\frac{dP_B}{dx}\right|_{x=0} + \lambda[P_A(0) - P_B(0)] = 0, \tag{d4}$$

where λ is the coupling coefficient. The periodic boundary conditions for the polarizations of an infinite superlattice structure can be described by

$$\kappa_A \left.\frac{dP_A}{dx}\right|_{x=-d_A} - \lambda[P_A(-d_A) - P_B(-d_A)] = 0,$$

$$\kappa_B \left.\frac{dP_B}{dx}\right|_{x=d_B} - \lambda[P_A(d_B) - P_B(d_B)] = 0, \tag{d5}$$

where d_A and d_B are the layer thicknesses of a bilayer unit.

The boundary conditions for the susceptibilities at the interfaces $x=0$ are

$$\kappa_A \left.\frac{d\chi_A}{dx}\right|_{x=0} - \lambda[\chi_A(0) - \chi_B(0)] = 0,$$

$$\kappa_B \left.\frac{d\chi_B}{dx}\right|_{x=0} + \lambda[\chi_A(0) - \chi_B(0)] = 0, \tag{d6}$$

and the periodic boundary conditions for the susceptibilities of an infinite superlattice structure can be described by

$$\kappa_A \left.\frac{d\chi_A}{dx}\right|_{x=-d_A} - \lambda[\chi_A(-d_A) - \chi_B(-d_A)] = 0,$$

$$\kappa_B \left.\frac{d\chi_B}{dx}\right|_{x=d_B} - \lambda[\chi_A(d_B) - \chi_B(d_B)] = 0. \tag{d7}$$

The boundary condition equations above are obtained by including an interfacial coupling energy term into the free energy and then minimizing the free energy of the interface

structure under applied electric field. The parameter λ describes the strength of the interfacial coupling between the constituents A and B. The detailed discussion about the interfacial coupling can be found in Refs. 14 and 15.

The average polarization P_{ave} and dielectric susceptibility χ_{ave} of the superlattice can be obtained as

$$P_{\text{ave}} = \frac{1}{L}\int_{-d_A}^{d_B} P(x)dx \tag{8}$$

and

$$\frac{1}{1+\chi_{\text{ave}}} = \frac{1}{L}\int_{-d_A}^{d_B} \frac{1}{1+\chi(x)}dx, \tag{9}$$

where $L=d_A+d_B$.

In our previous study of compositionally graded ferroelectric films,[8–10] we used the following formula for the time-dependent conductivity associated with space charges (TDSCL):

$$\sigma(x,t) = \frac{\mu_p - \mu_n}{2}\frac{\partial D(x,t)}{\partial x} + \sqrt{\left[\frac{\mu_p + \mu_n}{2}\frac{\partial D(x,t)}{\partial x}\right]^2 + \sigma_0(x)^2}, \tag{10}$$

where $D(x,t)=\varepsilon(x)E(x,t)+P(x,t)$ is the electric displacement at position x and time t, $\sigma_0(x)$ is the intrinsic conductivity, and μ_p and $-\mu_n$ ($\mu_p, \mu_n > 0$) are the positive and negative charge carrier mobilities, respectively. The concept of TDSCL conduction was first introduced to account for the well-known observation of polarization offsets in compositionally graded ferroelectric films, and subsequently it was found to have a wider applicability in explaining the imprint phenomenon commonly observed in homogeneous ferroelectric films.[8–10] Here we also propose to study the effect of taking this conduction mechanism into account to investigate the anomalous ferroelectric and dielectric behaviors of ferroelectric superlattices. The total current $J(t)$ across the superlattice structure is constitutive of the conduction and displacement currents,

$$J(t) = j_c(x,t) + j_d(x,t) = \sigma(x,t)E(x,t) + \frac{\partial}{\partial t}D(x,t), \tag{11}$$

where subscripts c and d denote the conduction and displacement parts, respectively. The circuit condition is given by

$$\int_{-d_A}^{d_B} E(x,t)dx = E(t)L, \tag{12}$$

where L is the period thickness, and $E(t)=E_{\text{amp}}\sin(\omega t)$ is the applied electric field across the superlattice. It is noted that the applied electric field amplitude E_{amp} should be sufficiently small so that polarization switching will not occur within the ferroelectric superlattice when measuring permittivity. The measured electric displacement of the superlattice at a certain time t is given by the integration of total current density across the circuit,

TABLE I. The dimensionless parameters used in our calculations.

Figure	d_A	d_B	$\kappa_A=\kappa_B$	λ
2(a)	Varied	Varied	10	Varied
2(b)	Varied	Varied	10	2.86
3	50	50	10	Varied
4(a)	90	10	100	100
4(b)	90	10	100	Varied
5	50	50	10	1
6	50	50	10	1

$$D(t) = \int_0^t J(t)dt. \tag{13}$$

Experimentally, the permittivity of the superlattice is

$$\varepsilon = \frac{\{D(t)\}_{\sin\omega t}}{E_{\text{amp}}}, \tag{14}$$

where $\{\}_{\sin\omega t}$ is the $\sin(\omega t)$—Fourier component of the function within the bracket.

III. RESULTS AND DISCUSSION

For simplicity the above variables are normalized into their dimensionless forms by the following relations:

$$D^* = \frac{D}{P_S}, \quad \varepsilon^* = \frac{\gamma\varepsilon}{\tau}, \quad j^* = \frac{\tau j}{P_S}, \quad \sigma^* = \gamma\sigma,$$

$$\mu_p{}^* = \frac{P_S\gamma\mu_p}{2\Delta x}, \quad \mu_n{}^* = \frac{P_S\gamma\mu_n}{2\Delta x}, \quad P^* = \frac{P}{P_S}, \quad t^* = \frac{t}{\tau},$$

$$x^* = \frac{x}{\Delta x}, \quad \lambda^* = \frac{\tau\lambda}{\gamma\Delta x}, \quad \alpha^* = \frac{\tau\alpha}{\gamma}, \quad \beta^* = \frac{\tau P_S^2\beta}{\gamma},$$

$$E^* = \frac{\tau E}{\gamma P_S}, \quad \kappa^* = \frac{\tau\kappa}{\gamma}, \tag{15}$$

where P_S is the remanent polarizations, Δx is a characteristic length, and τ is a characteristic relaxation time for the system.

The corresponding smallest realistic layer thickness in the present work would range approximately from 2 to 10 nm for different materials to ensure that the Landau continuum theory can be applied. We first study the intrinsic average polarization and dielectric susceptibility as a function of period thickness and the spatial dependence of the polarization and dielectric susceptibility for both "symmetric" and "asymmetric" superlattices. To gain more insight into the interplay of the effects of interfacial coupling and electrical conductivity, the dynamic ferroelectric and dielectric properties of the superlattices are also studied under the application of an external sinusoidal electric field. In the investigation the layer thickness d, interfacial coupling λ, and intralayer coupling κ parameters are varied as listed in Table I. The following parameters have been retained for obtaining all the results presented in this paper: $\alpha_A=-1$, $\beta_A=1$, μ_{pA}

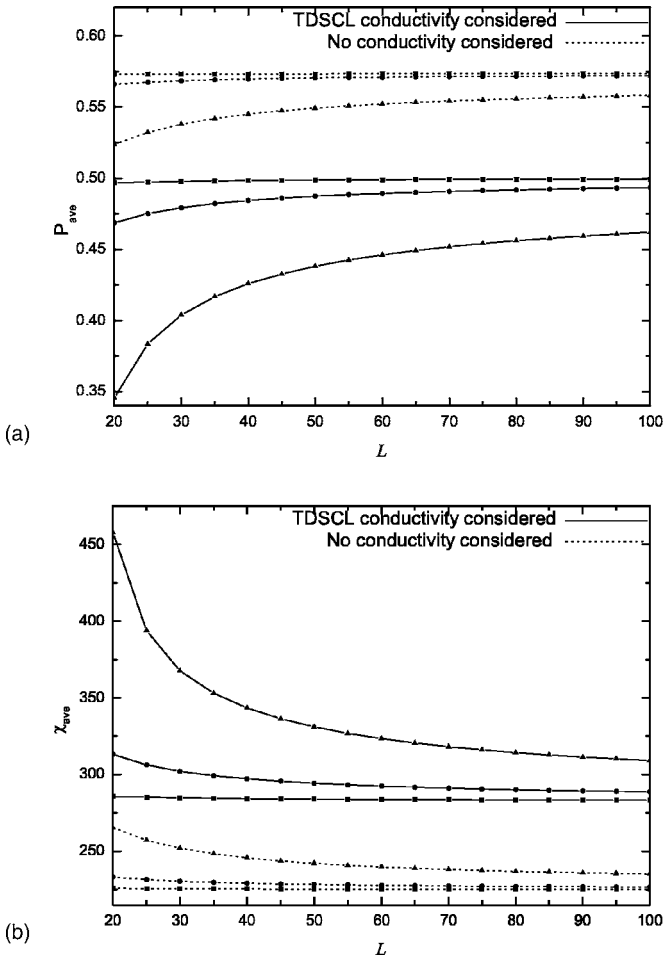

FIG. 2. Average polarization (a) and dielectric susceptibility (b) as a function of period thickness for a ferroelectric-paraelectric superlattice structure with different interfacial coupling strengths, taking TDSCL conducitivity into account or treating the superlattice as perfect insulator.

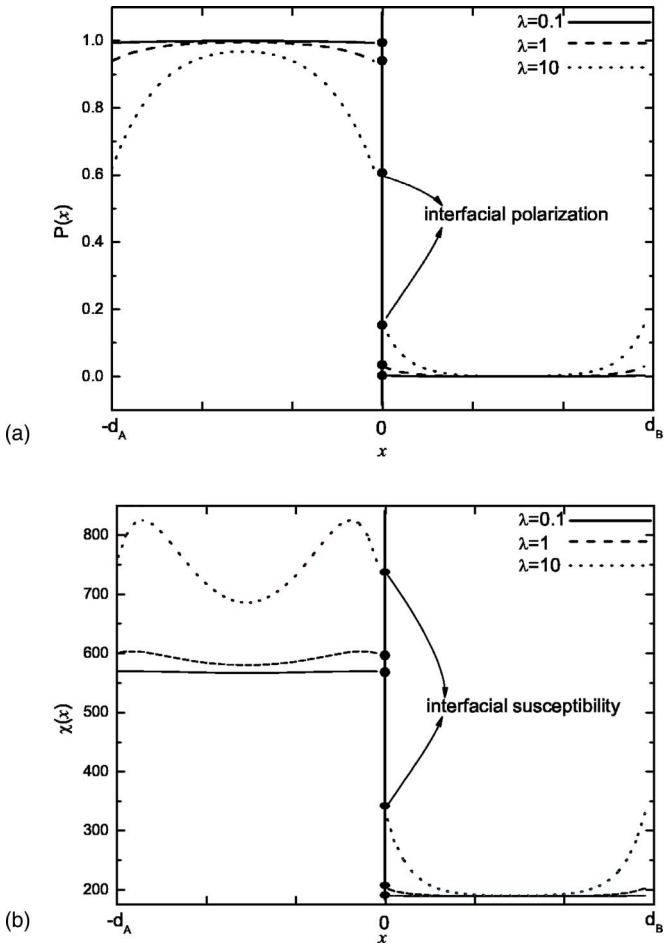

FIG. 3. Spatial dependence of polarization (a) and dielectric susceptibility (b) for a ferroelectric-paraelectric superlattice structure with different interfacial coupling strengths.

$=\mu_{nA}=1$, and $\sigma_{0A}=0.001$ for the ferroelectric layer; $\alpha_B=6$, $\beta_B=1$, $\mu_{pB}=\mu_{nB}=1$, and $\sigma_{0B}=0.0003$ for the paraelectric layer.

Figure 2 shows the intrinsic average polarization (a) and average susceptibility (b) as function of period thickness L of the superlattice by taking TDSCL conductivity into account (denoted by the solid lines) or treating the superlattice as perfect insulator (denoted by the dotted lines) for three different interfacial coupling strengths [in the figure, the values for λ are 0.1 (■), 1 (●), and 10 (▲)] without external electric field. It is shown that the average polarization of the interface-coupled superlattice will be reduced [see Fig. 2(a)] while the average susceptibility will be enhanced [see Fig. 2(b)] with increasing interfacial coupling strength, for both TDSCL conductivity and zero conductivity. The calculated trends are consistent with the reported results of the thickness induced transition.[7,16,17] Interestingly, the effect of interfacial coupling is more significant for short-period superlattice. It is also very interesting to note that the period thickness dependences of average polarization and susceptibility are more significant when considering TDSCL conductivity than treating the superlattice as an insulator, which become much more noticeable for stronger interfacial coupling, e.g., $\lambda=10$.

In order to gain more insight on the correlation between the interface structures and the properties of the ferroelectric-paraelectric superlattices, it would be much beneficial to look at the local polarization and dielectric responses of the superlattices. Figure 3 shows the spatial variation of polarization (a) and dielectric susceptibility (b) of a ferroelectric-paraelectric superlattice considering the effect of electrical conductivity. Generally, the existence of the interfacial coupling leads to the inhomogeneity of polarization across the interface between the ferroelectric and paraelectric layers.[14,15,18] The interface structure in the ferroelectric-paraelectric superlattice corresponds to the region near the interface between the ferroelectric and paraelectric layers in which the inhomogeneity of polarization took place. The interface structure exhibits a typical feature that the polarization of the ferroelectric layer near the interface is suppressed, whereas there is induced polarization near the interface of the paraelectric layer. With increasing coupling strength, this induced polarization is enhanced, and the polarization profile near the interface is more "bent." On the other hand, it is shown from Fig. 3(b) that the interfacial coupling leads to an enhancement of the local dielectric response near the interface. The enhancement of the local dielectric susceptibility near the interface is increased with increasing interfacial coupling strength. It is interesting to note that the susceptibility

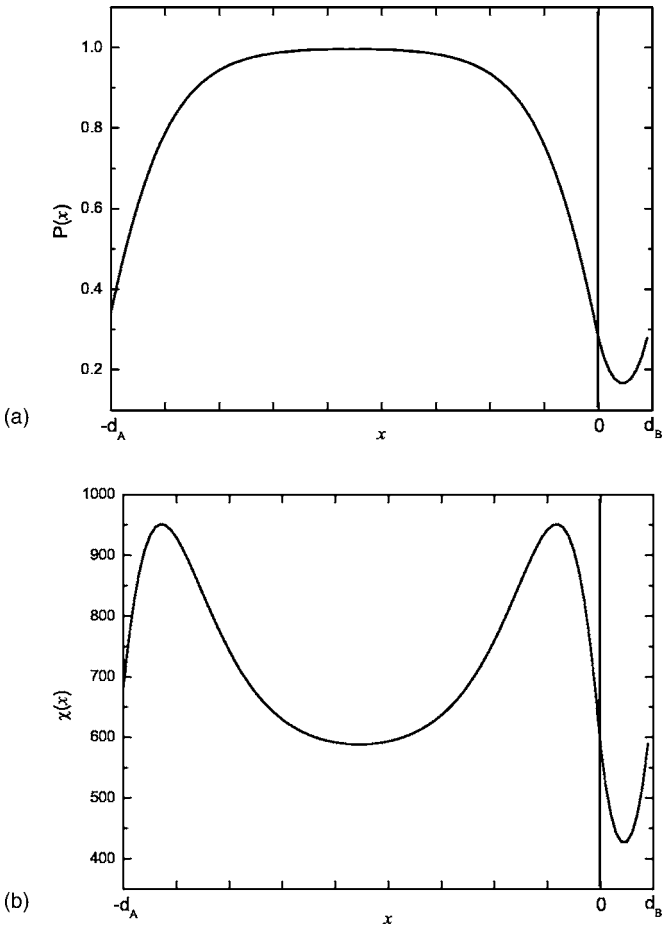

FIG. 4. Spatial dependence of polarization (a) and dielectric susceptibility (b) for an "asymmetric" ferroelectric-paraelectric superlattice with a larger local interaction coefficient κ and stronger interfacial coupling strength λ.

of the ferroelectric layer is more significantly enhanced than the susceptibility of the paraelectric layer, in particular, for stronger interfacial coupling, e.g., when $\lambda=10$ (more deviated from the bulk values of the individual components: 566 for the ferroelectric layer and 189 for the paraelectric layer in the calculation). It is interesting to note that the calculation will give similar spatial polarization and susceptibility profiles but with quite smaller magnitudes for local susceptibilities of the ferroelectric layers without considering conductivity.

Figure 4 shows the spatial variation of polarization (a) and dielectric susceptibility (b) of an asymmetric ferroelectric-paraelectric superlattice ($d_A \neq d_B$) with a larger local interaction coefficient κ and stronger interfacial coupling strength λ (see Table I) by taking electrical conductivity into account. It can be seen that the curves of both polarization and susceptibility are more seriously bent than the symmetric superlattice ($d_A=d_B$) with a weaker coupling as shown in Fig. 3. The interfacial values for polarization and susceptibility of the ferroelectric and paraelectric layers ($P(x)|_{x=0}$ and $\chi(x)|_{x=0}$) become identical. The most striking result is that there is a remarkable enhancement for the overall dielectric susceptibility with $\chi_{\text{ave}}=681$, which is much larger than those of the ferroelectric phase ($\chi_A=566$) and the paraelectric phase ($\chi_B=189$). This anomalous intrinsic dielectric property of the ferroelectric dielectric cannot be explained by the conventional capacitor series model, according to which the effective dielectric constant can be expressed as $1/\varepsilon_{\text{eff}}=[(d_A/\varepsilon_A)+(d_B/\varepsilon_B)]/(d_A+d_B)=472$. So the enhancement of the intrinsic dielectric permittivity is as high as 44%. It is worth noting that the calculation will give a value of 485 for the susceptibility if the superlattice is assumed to be insulating, which is not too different from 472. Therefore, it has been numerically validated that a larger thickness ratio d_A/d_B, a larger local interaction coefficient between neighboring layers κ, and a stronger interfacial coupling strength λ can generally significantly enhance the overall dielectric response for a ferroelectric-paraelectric superlattice, which is consistent with other theoretical predictions based on transverse Ising model (TIM).[16]

The above results have described the static ferroelectric and dielectric behaviors of both symmetric and asymmetric ferroelectric-paraelectric superlattices, which are obtained by allowing the system to relax from a convenient initial condition to the equilibrium condition (time independent, with $\partial/\partial t=0$). It is found that the same equilibrium state is reached even when TDSCL conductivity is reduced to the Ohmic conductivity. In fact, it is more important to study the dynamic properties of the superlattices because the experimental data are obtained under dynamic measurements. So only the determination of remanent polarization from the calculated dynamic *D-E* (often called *P-E*) hysteresis loop can be directly compared with experimental P_r, which is usually measured from hysteresis loops under the application of external cyclic electric fields.

Figure 5 shows the *P-E* relations of the ferroelectric layer, paraelectric layer, and the superlattice simulated by taking Ohmic conductivity into account (a) and by considering TDSCL conductivity (b). There is almost no hysteresis behavior for the *P-E* relations of the paraelectric layer as expected (see the dashed line). The remanant polarization (P_r) and coercive field (E_c) of the superlattice (see the solid line) are much smaller than the P_r and E_c values of the ferroelectric layer (see the dotted line) when only Ohmic conductivity is considered, where $\sigma_{0A}=0.001$ and $\sigma_{0B}=0.0003$ [Fig. 5(a)], due to the existence of the paraelectric layer. We have also tried different Ohmic conductivity magnitudes and it is found that the superlattice P_r and E_c will always be smaller than that of the ferroelectric layer, although the hysteresis loops indeed demonstrate a leaky characteristic for larger conductivity values. On the other hand, it is very interesting to note that the hysteresis loop of the superlattice becomes much more inflated when taking TDSCL conductivity into account [the solid line in Fig. 5(b)]. It is also remarkable to note that the P_r and E_c values of the superlattice in this case are larger than the P_r and E_c values of the ferroelectric layer. The characteristics of this inflated loop are very similar with those of the experimentally observed loops of the ferroelectric-paraelectric superlattices.[1,2]

Figure 6 shows the frequency dependence of the dielectric permittivity of the superlattice calculated by taking Ohmic conductivity into account (denoted by the dotted line), where $\sigma_{0A}=0.001$ and $\sigma_{0B}=0.0003$, and by considering TDSCL conductivity (the solid line). The frequency dependence of the dielectric permittivity is due to the involvement

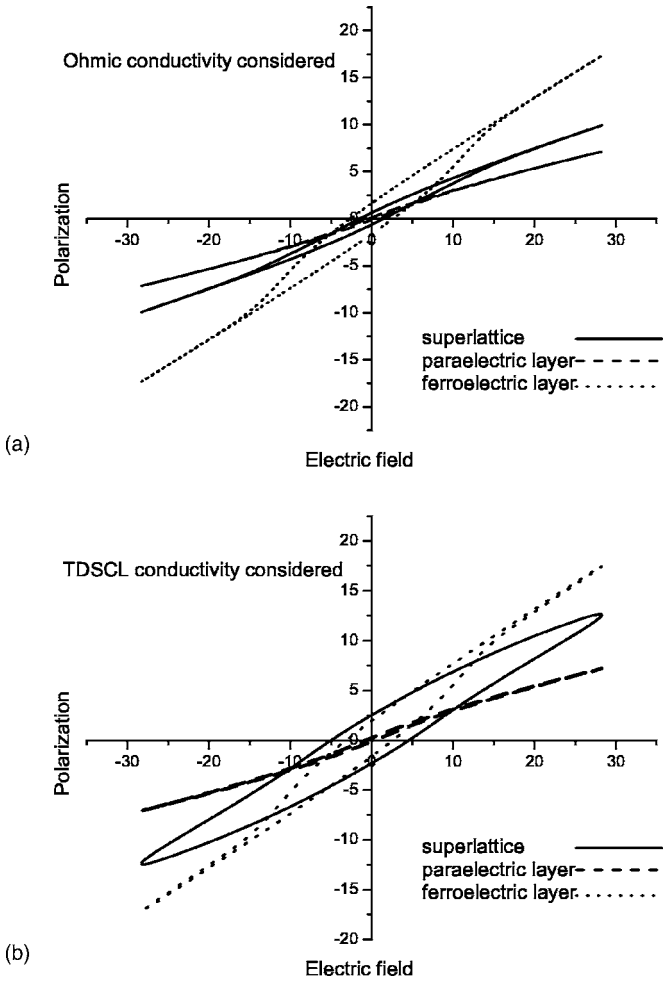

FIG. 5. Calculated *P-E* relations of ferroelectric layer, paraelectric layer, and the superlattice, considering only Ohmic conductivity (a) and considering TDSCL conductivity (b).

of electrical conductivity. The calculated dielectric permittivity decreases with increasing frequency f as shown in Fig. 6, a trend also experimentally observed in many ferroelectric superlattices.[2,5] In addition, we have also tried different

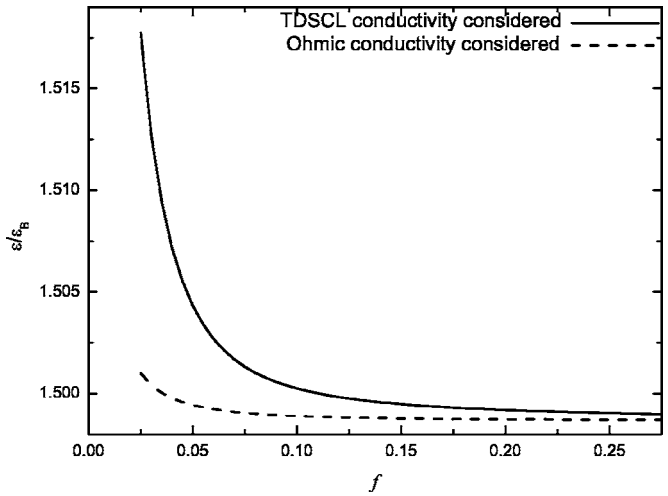

FIG. 6. Frequency dependence of calculated permittivity of the superlattice, considering only Ohmic conductivity (denoted by the dotted line) and considering TDSCL conductivity (denoted by the solid line).

Ohmic conductivity magnitudes and it is found that the ε-f curve becomes more bent when considering TDSCL conductivity than that of considering Ohmic conductivity, particularly at lower frequency.

From the above results, we see that TDSCL conductivity is a requisite for the enhancement of remanent polarization which cannot be obtained by considering only Ohmic conductivity. Although the consideration of the TDSCL conduction is not a requisite for the enhancement of permittivity in all cases, it is likely to be one of the important factors to be included in understanding the anomalous dielectric behaviors of the ferroelectric-paraelectric superlattices where large permittivity enhancement is observed in experiments. In addition, it has been numerically validated that the effect of interfacial coupling strength becomes insignificant for the dynamic ferroelectric and dielectric properties of the superlattices with relatively large period thickness, e.g., $\geqslant$10 nm. Interestingly, it is found that the calculated hysteresis loops will indeed become a bit inflated for very short-period superlattice, e.g., L=2 nm, with stronger interfacial coupling.

Summing up, we first study the intrinsic polarization and dielectric response of a periodic ferroelectric superlattice consisting of alternating ferroelectric and paraelectric layers with interfacial coupling. The average dielectric properties would be much enhanced for the slightly conducting superlattices compared to the insulating ones. Both the symmetric and asymmetric superlattice structures are studied and it is found that the intrinsic polarization and dielectric response would be very sensitively dependent on the period thickness, thickness ratio, local interaction coefficients, and the interfacial coupling strength of the ferroelectric and dielectric layers. In particular, it has been demonstrated that a remarkable enhancement of intrinsic dielectric susceptibility can be obtained by decreasing the period thickness, modulating the thickness ratio, and increasing the local interaction coefficients and the interfacial coupling strength. On the other hand, the simulated hysteresis loop of the superlattice will become much inflated, thus giving a larger remanent polarization value than the single-phase ferroelectric layer, which cannot be satisfactorily explained by traditional theoretical models either treating the superlattice as perfectly insulating or taking only Ohmic conductivity into account.

All in all, we have developed a continuum model based on the Landau-Ginzburg theory to study the ferroelectric and dielectric behaviors of the ferroelectric-paraelectric superlattices with layer thicknesses larger than the characteristic continuum limits, where the continuum theory can still be utilized. A good understanding of the anomalous ferroelectric and dielectric behaviors of the superlattices is obtained and some key experimental features are reproduced by our model, which we believe has clarified and furnished a deeper understanding of the effects of interface structure and TDSCL conductivity and should be very significant for device design and optimization of some ferroelectric superlattice structures.

ACKNOWLEDGMENT

The work described in this article is supported by a Hong Kong Polytechnic University internal grant. Special

thanks are due to Dr. K. H. Chew from The Hong Kong Polytechnic University for motivating the work on superlattice, Dr. H. K. Chan from The University of Manchester, UK for his helpful discussion.

[1]T. Shimuta, O. Nakagawara, T. Makino, S. Arai, H. Tabata, and T. Kawai, J. Appl. Phys. **91**, 2290 (2002).
[2]F. M. Pontes, E. Longo, E. R. Leite, and J. A. Varela, Appl. Phys. Lett. **84**, 5470 (2004).
[3]H. N. Lee, H. M. Christen, M. F. Chisholm, C. M. Rouleau, and D. H. Lowndes, Nature (London) **433**, 395 (2005).
[4]R. Xu, M. R. Shen, S. B. Ge, Z. Q. Gan, and W. W. Cao, Thin Solid Films **406**, 113 (2002).
[5]C. Wang, Q. F. Fang, Z. G. Zhu, A. Q. Jiang, S. Y. Wang, B. L. Cheng, and Z. H. Chen, Appl. Phys. Lett. **82**, 2880 (2003).
[6]M. Sepliarsky, S. R. Phillpot, M. G. Stachiotti, and R. L. Migoni, J. Appl. Phys. **91**, 3165 (2002).
[7]B. D. Qu, W. L. Zhong, and R. H. Prince, Phys. Rev. B **55**, 11218 (1997).
[8]H. K. Chan, C. H. Lam, and F. G. Shin, J. Appl. Phys. **95**, 2665 (2003).
[9]Y. Zhou, H. K. Chan, C. H. Lam, and F. G. Shin, J. Appl. Phys. **98**, 034105 (2005).
[10]Y. Zhou, H. K. Chan, C. H. Lam, and F. G. Shin, J. Appl. Phys. **98**, 024111 (2005).
[11]C. K. Wong and F. G. Shin, J. Appl. Phys. **97**, 064111 (2005).
[12]L. Baudry and J. Tournier, J. Appl. Phys. **90**, 1442 (2001).
[13]L. Baudry, J. Appl. Phys. **86**, 1096 (1999).
[14]C. H. Tsang, K. H. Chew, Y. Ishibashi, and F. G. Shin, J. Phys. Soc. Jpn. **73**, 3158 (2004).
[15]K. H. Chew, Y. Ishibashi, and F. G. Shin, J. Phys. Soc. Jpn. **74**, 2338 (2005).
[16]K. H. Chew, Y. Ishibashi, and F. G. Shin, J. Phys. Soc. Jpn. (submitted).
[17]Y. Q. Ma, J. Shen, and X. H. Xu, Solid State Commun. **114**, 461 (2000).
[18]K. H. Chew, Y. Ishibashi, F. G. Shin, and H. L. W. Chan, J. Phys. Soc. Jpn. **72**, 2364 (2003).